# Kinetic Mechanism for p38 MAP Kinase

Philip V. LoGrasso,* Betsy Frantz, Anna M. Rolando, Stephen J. O'Keefe, Jeffery D. Hermes, and Edward A. O'Neill

*Departments of Molecular Design and Diversity and of Immunology and Inflammation, Merck Research Laboratories, P.O. Box 2000, Rahway, New Jersey 07065*

*Received March 24, 1997; Revised Manuscript Received June 9, 1997*[⊗]

ABSTRACT: p38 has been shown to be a critical enzyme in the pro-inflammatory cytokine pathway and is a member of the mitogen-activated protein (MAP) kinase family. While the details for p38 activation and subsequent signal transduction have begun to be elucidated, little is known about the kinetic mechanism for p38. In this study, we have determined the kinetic mechanism for p38 MAP kinase. Data from initial velocity patterns in the presence and absence of a dead-end inhibitor and two triarylimidazole p38 inhibitors were consistent with an ordered sequential mechanism for p38 with protein substrate, glutathione *S*-transferase-activating transcription factor 2 (GST-ATF2), binding before ATP. The ATP analog, adenylyl methylenediphosphonate (AMP-PCP), and two triarylimidazoles were competitive inhibitors versus ATP and uncompetitive inhibitors versus GST-ATF2. Equilibrium binding studies utilizing a tritiated ATP-competitive inhibitor were also consistent with this mechanism and suggest an inability of ATP to bind to p38 in the absence of protein substrate. Moreover, the Michaelis constant for GST-ATF2 was 12-fold greater than the dissociation constant, indicating that the binding of ATP affected the binding of GST-ATF2. An ordered sequential mechanism with protein substrate binding first is unique to p38 compared to cyclic AMP-dependent protein kinase (cAPK) and most tyrosine kinases and helps to explain the interaction between enzyme, substrates, and inhibitors.

The biochemical pathways for the inflammatory response mediated through the activation of mitogen-activated protein (MAP)[1] kinases have generated a great deal of interest in the past several years. A number of reports describe the role of MAP kinases in cellular processes such as cell proliferation, response to environmental stress, and cell death (Han et al., 1994; Raingeaud et al., 1995; Johnson et al., 1996; Lee & Young, 1996). The focus of our study was on p38; a MAP kinase first shown to be phosphorylated and activated in response to lipopolysaccharide (LPS, or endotoxin) (Han et al., 1993). Besides LPS, subsequent studies have shown that other environmental stimuli such as TNFα, IL-1$\beta$, and hyperosmolality each lead to activation of p38 (Han et al., 1994; Raingeaud et al., 1995). In 1994, Lee et al., utilizing a combination of binding assays, photoaffinity labeling, cDNA cloning, and biochemical characterization experiments, identified p38 MAP kinase as a critical enzyme involved in the regulation of inflammatory cytokine biosynthesis. Moreover, they showed that p38 could be potently and specifically inhibited *in vitro* and *in vivo* by a series of pyridinylimidazoles (Lee et al., 1993; Cuenda et al., 1995), thereby leading to inhibition of cytokine production. While some of the details for many of the above processes are known, there are no studies that have investigated the kinetic mechanism of p38.

In 1982, Cook et al. reported that the kinetic mechanism for cAMP-dependent protein kinase (cAPK), a Ser/Thr kinase family member, proceeded by a random addition of substrates and an ordered release of products. In contrast, Whitehouse et al. (1983) suggested a steady-state ordered sequential mechanism for cAPK with ATP binding first. The kinetic mechanisms for several tyrosine kinases have also been reported. Results from steady-state kinetic analysis of human c-terminal src kinase (csk) support either a random sequential mechanism or an ordered mechanism in which ATP binds before poly(Glu,Tyr) (Cole et al., 1994). Steady-state data for pp60 c-src utilizing a synthetic peptide showed a random sequential kinetic mechanism (Boener et al., 1995). Like cAPK, two different mechanisms have been reported for the epidermal growth factor receptor (EGFR). Posner et al. (1992) described a rapid equilibrium random sequential mechanism for EGFR utilizing either poly($Glu_6Ala_3Tyr$) or $Val^5$-angiotensin II as substrate. On the other hand, Erneux et al. (1983) reported an ordered sequential mechanism for EGFR with synthetic peptide substrate binding before ATP.

The current study was designed to investigate the kinetic mechanism for p38 MAP kinase. Steady-state kinetic analysis of the incorporation of $^{33}P$-labeled phosphate into GST-ATF2 was utilized to monitor catalysis. The ATP analog adenylyl methylenediphosphonate (AMP-PCP) and two triarylimidazole p38 inhibitors were utilized to determine the mode of inhibition versus GST-ATF2 and ATP. The major finding of this study was that the kinetic mechanism for p38 MAP kinase proceeded by a rapid-equilibrium ordered sequential mechanism with protein substrate, GST-

* To whom correspondence should be addressed at Merck Research Laboratories, P.O. Box 2000, Building R50A-300, Rahway, NJ 07065. Phone: (908)594-1271. Electronic mail address: lograsso@merck.com.

[⊗] Abstract published in *Advance ACS Abstracts,* August 15, 1997.

[1] Abbreviations: AMP-PCP, adenylyl methylenediphosphonate; ATF-2, activating transcription factor 2; BSA, bovine serum albumin; cAPK, cyclic AMP-dependent protein kinase; Csk, c-terminal pp60c-src tyrosine kinase; DTT, dithiothreitol; EDTA, ethylenediaminetetraacetic acid; EGFR, epidermal growth factor receptor; ERK-2, extracellular-regulated protein kinase 2; GST, glutathione *S*-transferase; HEPES, *N*-(2-hydroxyethyl)piperazine-*N*′-2-ethanesulfonic acid; IL-1, interleukin-1; LPS, lipopolysaccaride; MAP, mitogen-activated protein kinase; PKI, cAPK inhibitor peptide; src, pp60c-src tyrosine kinase; TNF, tumor necrosis factor.

S0006-2960(97)00677-6 CCC: $14.00 

ATF2, binding before ATP. Furthermore, the data were consistent with GST-ATF2 and ATP being interacting substrates and suggest that ATP binds very poorly to p38 in the absence of protein substrate.

## MATERIALS AND METHODS

*Expression and Purification of p38 and GST-ATF2.* cDNA encoding p38 was generated from human T cell RNA using the GeneAmp protocol (Perkin Elmer). The cDNA was modified to encode an N-terminal FLAG epitope (Kodak) and was cloned into plasmid pRMHA-3 (derived from pRmHA-1; Bunch et al., 1988) under transcriptional control of a copper-inducible metallothionein promoter. The new plasmid (pRM-h38a) was cotransfected with a neomycin resistance plasmid, pS2-neo (derived from pUChsneo; Steller & Pirrotta, 1985), into *Drosophila* Schneider S2 cells, and clonal selection in 1.5 mg/mL active G418 for stable transfectants was carried out. The p38-S2 line was chosen from among 38 candidate clones by virtue of its relatively high level of Flag-p38 expression as measured by Western blot analysis. S2 cells were grown in Schneider's *Drosophila* medium (Gibco) supplemented with 10% fetal calf serum (Biocell), 50 $\mu$g/mL gentamicin (Gibco), and 2 mM glutamate (Gibco) to a density of $2 \times 10^6$ cells/mL in 1 L spinner flasks at 30 °C. Expression of recombinant p38 was induced by treating transfected cells with 1 mM $CuSO_4$ for 4 h. To induce phosphorylation of recombinant p38, $CuSO_4$-induced cells were stimulated 10 min prior to harvest with 400 mM NaCl, 2 mM $Na_3VO_4$, and 100 $\mu$g/L okadaic acid. Cell pellets from 2 L of cells were washed with PBS, 2 mM $Na_3VO_4$, and lysed in 20 mM Tris, pH 7.5, 120 mM NaCl, 1% Triton X-100, 2 mM EDTA, 20 mM NaF, 4 mM $Na_3VO_4$, and 2 mM Pefabloc SC (Boehringer Mannheim). Extracts were centrifuged for 10 min at 13000*g*, and p38 from a 30 mL lysate was immunoaffinity-purified by column chromatography through 2.5 mL of packed anti-FLAG M2 resin (Kodak). The affinity resin was equilibrated with lysis buffer. After the extract was loaded, the resin was washed with 10 column volumes of lysis buffer, 10 column volumes of buffer A (10 mM Tris, pH 7.5, 500 mM NaCl, and 20% glycerol), and then 10 column volumes of buffer B (10 mM Tris, pH 7.5, 150 mM NaCl, and 20% glycerol). The fusion protein was eluted in buffer B containing 100 $\mu$g/mL FLAG peptide.

cDNA encoding the N-terminal 115 amino acids of ATF2 was generated from human brain poly(A)RNA (Clonetech) and cloned in pGEX-5X-1(Pharmacia) as a GST fusion protein. The resulting plasmid, pGST-ATF2, was transfected into BL21(DE3 pLys S) cells (Novagen). Expression of GST-ATF2 protein was induced by treating the cells for 2 h with 1 mM IPTG. The protein was purified over glutathione−agarose according to standard procedures (Pharmacia).

*Steady-State Kinetics.* Initial velocity studies utilized to determine the steady-state constants for ATP and GST-ATF2 were carried out in 100 $\mu$L volumes containing the final concentrations of the following: 25 mM HEPES (Sigma) (pH 7.4); 10 mM $MgCl_2$ (Sigma); 2 mM DTT (Sigma); 20 mM $\beta$-glycerophosphate (Sigma); 0.1 mM $Na_3VO_4$ (Sigma); 4 $\mu$Ci of [$\gamma$-$^{33}$P]ATP (2000 Ci/mmol; 1 Ci = 37 GBq) (Amersham); 2.5−250 $\mu$M ATP (Pharmacia); and 1.16−11.6 $\mu$M GST-ATF2. Buffer composition was optimized for pH and DTT and $MgCl_2$ concentrations. $MgCl_2$ was varied from 1 to 100 mM. The $MgCl_2$ concentration which gave maximal velocity was between 10 and 30 mM. The reactions were initiated with the addition of 5 nM p38 (final concentration) and incubated for 60 min at 30 °C. Under these conditions, less than 10% of substrate was converted to product. Moreover, aliquots taken at 0, 10, 20, 30, 40, and 60 min revealed that the reaction was linear for this time course over the entire range and combination of substrate concentrations: [GST-$ATF_2$] = 11.6 $\mu$M/[ATP] = 250 $\mu$M (correlation coefficient = 0.999); [GST-$ATF_2$] = 11.6 $\mu$M/[ATP] = 2.5 $\mu$M (correlation coefficient = 0.997); [GST-$ATF_2$] = 0.58 $\mu$M/[ATP] = 2.5 $\mu$M (correlation coefficient = 0.997). Reactions were stopped with 100 $\mu$L of 100 mM EDTA/15 mM sodium pyrophosphate. Fifty microliters of the stopped reaction was spotted in triplicate on a 15 mM sodium pyrophosphate-pretreated phosphocellulose 96-well plate (Millipore MAPHNOB 10). The samples were vacuum-filtered and washed 3 times each with 100 $\mu$L of 75 mM $H_3PO_4$ to remove excess [$\gamma$-$^{33}$P]ATP. After washing and a final filtration step to remove $H_3PO_4$, 50 $\mu$L of Microscint-20 (Packard) was added to each well, and samples were analyzed on a Packard Topcount liquid scintillation counter. All enzyme reactions were performed at least twice. The initial velocities as a function of both GST-ATF2 and ATP concentrations were fitted to equations for ternary complex (sequential) and ping-pong mechanisms (Leatherbarrow, 1992). Kinetic constants were determined from nonlinear least-squares analysis (Leatherbarrow, 1992).

*Enzyme Inhibition.* Enzyme inhibition studies were performed as described for two-substrate kinetics. When ATP was the varied substrate, [GST-ATF2] was fixed at 11.6 $\mu$M, and when GST-ATF2 was the varied substrate, [ATP] was fixed at 50 $\mu$M. For inhibition experiments, the concentration of AMP-PCP (Sigma) ranged from 25 $\mu$M to 2.5 mM; [SB 203580] ranged from 2 to 250 nM; and [SB 202190] ranged from 15 to 480 nM. The initial velocities were fitted to equations for competitive, uncompetitive, and full noncompetitive inhibition, and kinetic constants were determined from a nonlinear least-squares fit (Leatherbarrow, 1992). Reactions were spotted in triplicate, and inhibition reactions were performed twice for AMP-PCP and SB 203580 and once for SB 202190.

*Equilibrium Binding Assays.* Equilibrium binding of [2,6-$^3$H]-SB 202190 (71.4 mCi/mg) to p38 in the presence of GST-ATF2 or BSA was measured in 100 $\mu$L of a reaction mixture which contained 2 mM Tris (Digene) (pH 7.4), 5 mM mercaptoethanol (Sigma), 25 mM HEPES (pH 7.4), 10 mM $MgCl_2$, 2 mM DTT, 20 mM $\beta$-glycerophosphate, 0.1 mM $Na_3VO_4$, 17 nM [2,6-$^3$H]-SB 202190, 187 nM p38, 52 $\mu$M GST-ATF-2 or 50 $\mu$M BSA, and ATP from 10 $\mu$M to 5 mM. The mixture was incubated for 15 min at 30 °C; 45 $\mu$L was applied in duplicate to Centri-Sep (Princeton Separations) gel filtration columns (size exclusion limit ~25 kDa) that were prewashed with 0.8 mL of 2 mM Tris (pH 7.4) and 5 mM mercaptoethanol. p38-bound [2,6-$^3$H]-SB 202190 was separated from unbound [2,6-$^3$H]-SB 202190 by centrifugation at 700*g* for 2 min; 40 $\mu$L aliquots were added to 4 mL of Ultima Gold (Packard) scintillation fluid and counted using a Packard Tricarb 2500-TR liquid scintillation counter. Data presented are from the average of three experiments.

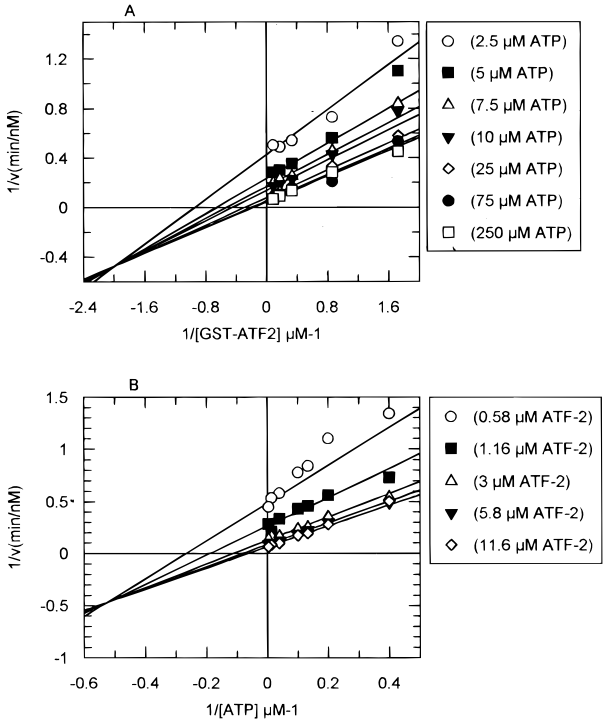


FIGURE 1: Two-substrate profile analysis for p38 MAP kinase. (A) Double-reciprocal plot of $1/v$ (min/nM) versus 1/[GST-ATF2] ($\mu M^{-1}$) at seven fixed ATP concentrations. (B) Double-reciprocal plot of $1/v$ (min/nM) versus 1/[ATP] ($\mu M^{-1}$) at five fixed GST-ATF2 concentrations. The data were fit to the equation for ternary complex formation (Leatherbarrow, 1992).

Table 1: Kinetic Constants for p38 MAP Kinase from Two-Substrate Kinetics[a]

| substrate | $K_m$ ($\mu$M) | $k_{cat}$ ($min^{-1}$) | $K_{ia}$ ($\mu$M) |
|---|---|---|---|
| GST-ATF2 | $6.2 \pm 0.6$ | $4.8 \pm 0.2$ | $0.5 \pm 0.3$ |
| MgATP | $23 \pm 2$ | | |

[a] The kinetic parameters were calculated from the equation for a ternary complex. The errors shown are standard errors. Data are from a single experiment performed in triplicate. Repeat experiments yielded identical results.

## RESULTS

*Initial Velocity Studies.* Two-substrate profile analysis was performed on activated p38 MAP kinase utilizing GST-ATF2 and ATP. Double-reciprocal plots of $1/v$ versus 1/[GST-ATF2] and $1/v$ versus 1/[ATP] are presented in Figure 1A and Figure 1B, respectively. Intersecting line patterns were observed, indicating a sequential kinetic mechanism. The steady-state kinetic constants generated from fitting the data to the equation for formation of a ternary complex are given in Table 1. The dissociation constant $K_{i\ GST-ATF2}$ was approximately 12-fold less than the corresponding $K_m$ value, indicating interactive substrate binding.

*Equilibrium Binding.* We were further able to probe how binding of protein substrate affected binding of ATP by utilizing equilibrium binding experiments. A useful compound for such experiments was reported by Lee et al. (1994) and is shown in Figure 2A. Scatchard analysis of SB 202190 by Lee et al. (1994) yielded a $K_d$ of 30−50 nM with a single binding site. In our experiments, we measured the ability of ATP to compete with SB 202190 for binding to p38 in the presence of GST-ATF2, a protein substrate, or BSA, a nonphosphorylatable protein as a control. The results are depicted in Figure 3 and revealed GST-ATF2 enhanced the ability of ATP to compete with SB 202190 for binding to p38 by 10-fold compared to BSA, a nonspecific protein carrier.

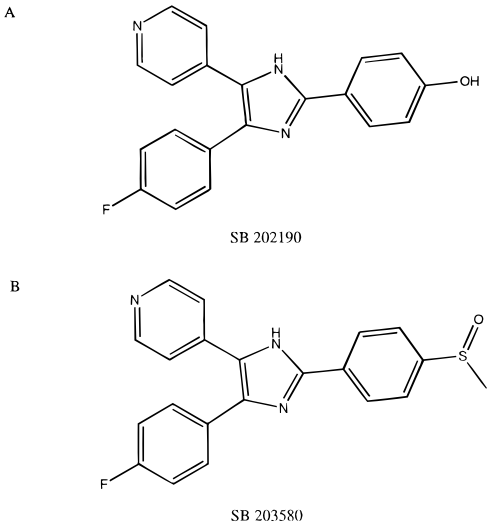


FIGURE 2: (A) Structure for SB 202190. (B) Structure for SB 203580.

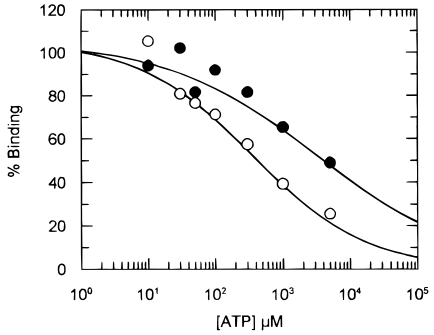


FIGURE 3: Equilibrium binding of ATP to p38 in the presence of GST-ATF2 (open circles) and BSA (filled circles): binding competition with [2,6-$^3$H]-SB 202190. Maximum cpm for binding of SB 202190 to p38 in the presence of GST-ATF2 = 10 000 and in the presence of BSA = 5000.

*Mode of Inhibition.* To extend the findings from the two-substrate profile analysis which showed that p38 MAP kinase proceeded by a sequential mechanism, we attempted to distinguish between random or ordered addition of substrates by investigating the mode of inhibition for the ATP analog, AMP-PCP, versus ATP or protein substrate, GST-ATF2. Analysis of kinetic data utilizing dead-end inhibitors has been shown to be valuable in determining and distinguishing kinetic mechanisms (Fromm, 1979). AMP-PCP was a competitive inhibitor versus ATP, having $K_{is} = 69 \pm 18\ \mu M$ (Figure 4A; Table 2), and an uncompetitive inhibitor versus GST-ATF2 (Figure 4B; Table 2). Comparison of the standard error analysis and regression analysis (reduced $\chi^2$) between the fits for competitive inhibition, full noncompetitive inhibition, and uncompetitive inhibition favors competitive inhibition for AMP-PCP versus ATP. Like analysis favors uncompetitive inhibition for AMP-PCP versus GST-$ATF_2$. These data are consistent with an ordered sequential kinetic mechanism for p38 with protein substrate binding before ATP (Scheme 1). These kinetic data are also consistent with our equilibrium binding studies (Figure 3)

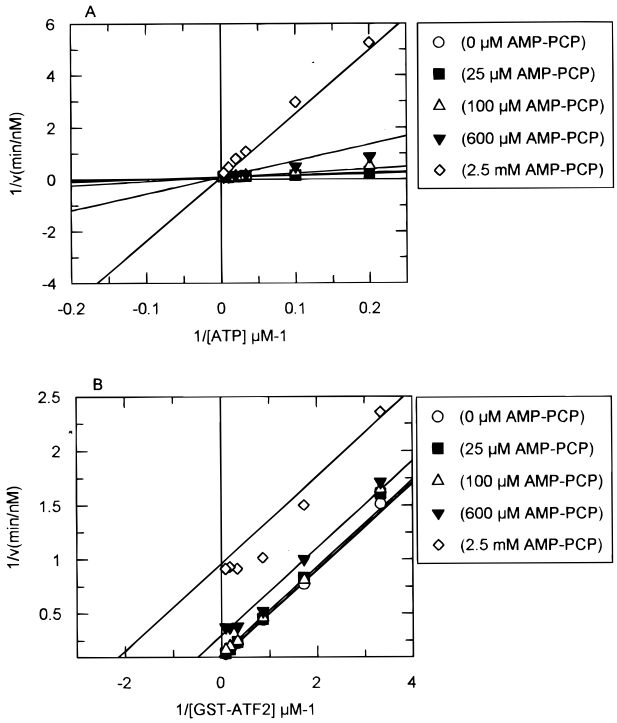


FIGURE 4: AMP-PCP inhibition of p38. (A) Double-reciprocal plot of $1/v$(min/nM) versus 1/[ATP] ($\mu M^{-1}$) performed at five fixed AMP-PCP concentrations. The GST-ATF2 concentration was fixed at 11.6 $\mu$M. The data were fit to the equation for competitive inhibition (Leatherbarrow, 1992). (B) Double-reciprocal plot of $1/v$ (min/nM) versus 1/[GST-ATF2] ($\mu M^{-1}$) at five fixed AMP-PCP concentrations. The ATP concentration was fixed at 50 $\mu$M. The data were fit to the equation for uncompetitive inhibition (Leatherbarrow, 1992).

Table 2: Inhibition Constants and Mode of Inhibition for p38 MAP Kinase[a]

| inhibitor | varied substrate | inhibition pattern | $K_{is}$ ($\mu$M) | $K_{ii}$ ($\mu$M) |
|---|---|---|---|---|
| AMP-PCP | GST-ATF2 | UC | | $274 \pm 20$ |
| SB 203580 | GST-ATF2 | UC | | $0.084 \pm 0.006$ |
| SB 202190 | GST-ATF2 | UC | | $0.063 \pm 0.005$ |
| AMP-PCP | ATP | C | $69 \pm 18$ | |
| SB 203580 | ATP | C | $0.034 \pm 0.002$ | |
| SB 202190 | ATP | C | $0.016 \pm 0.001$ | |

[a] Inhibition constants were calculated from the equation for either uncompetitive or competitive inhibition. The errors shown are standard errors. Data are from a single experiment performed in triplicate. Repeat experiments yielded identical results.

Scheme 1: Ordered Sequential Kinetic Mechanism for p38

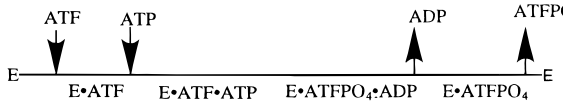


suggesting ATP can only bind to the E·GST-ATF2 complex and not free enzyme.

In an effort to understand the mechanism by which the triarylimidazoles inhibit p38, we investigated the mode of inhibition for SB 203580 (Figure 2B) which was reported to be a specific inhibitor of p38 MAP kinase (Cuenda et al., 1995). SB 203580 was a competitive inhibitor versus ATP, having $K_{is} = 34 \pm 2$ nM (Table 2), and an uncompetitive inhibitor versus GST-ATF2 (Table 2). Similar inhibition patterns were seen for SB 202190 versus ATP and GST-ATF2. The $K_{is}$ value for SB 202190 is given in Table 2.

## DISCUSSION

Our study focused on determining the kinetic mechanism for p38 MAP kinase, a member of the Ser/Thr protein kinase family. To date, there are no reports that examine the kinetic mechanism for any of the MAP kinases. Rather, mechanistic studies on cAPK have served as the paradigm for the Ser/Thr and consequently MAP kinase families (Cook et al., 1982; Whitehouse et al., 1983; Kong & Cook, 1988; Adams & Taylor, 1992). With a number of recent reports showing p38 to be a critical enzyme in pro-inflammatory cytokine biosynthetic pathways and cell proliferation (Han et al., 1994; Raingeaud et al., 1995; Lee & Young, 1996), an understanding of the kinetic mechanism for p38 MAP kinase will be useful.

Using a combination of initial velocity studies, equilibrium binding, and dead-end inhibition patterns (Figures 1, 3, and 4), we have generated a compelling set of data for p38 that suggests an ordered sequential kinetic mechanism whereby protein substrate binds first and is required for ATP binding. This is the first such report for this type of mechanism for a Ser/Thr protein kinase. The inhibition pattern for AMP-PCP versus ATP showed the characteristic intersecting line pattern for competitive inhibition (Segel, 1975; Figure 4A). This pattern was expected considering AMP-PCP differs in structure from ATP only by addition of a methylene group inserted between the $\beta$- and $\gamma$-phosphates of ATP. The parallel line pattern characteristic of uncompetitive inhibition (Segel, 1975; Figure 4B) was seen for the competition between AMP-PCP and GST-ATF2. Such a pattern would suggest that AMP-PCP can only bind to the E·GST-ATF2 complex. Indeed, when the data are fit to full noncompetitive inhibition, the $K_{is}$ term representing the E·I complex is very poorly defined ($3.1 \times 10^{18} \pm 2.1 \times 10^{18}$), indicating that AMP-PCP, like ATP, does not bind to free enzyme, but requires GST·ATF2 to be bound first.

The inhibition data for AMP-PCP also help to explain the observation from the initial velocity studies (Figure 1; Table 1) which demonstrated that GST-ATF2 and ATP were interacting sites. In many ways, the observation that the binding of protein substrate can affect the binding of ATP to p38 is very similar to that which was observed in the crystal structure of inhibitor peptide (PKI) and ATP-bound cAPK (Zheng et al., 1993). The crystal structure of the ternary complex revealed that the binding of PKI and MgATP is synergistic and that both $Mg^{2+}$ and ATP bind poorly to uncomplexed enzyme. Indeed, Whitehouse and Walsh (1983) showed a large increase in the affinity of MgATP for cAPK complexed with PKI compared to uncomplexed cAPK. While the observation that the protein substrate and ATP binding sites in p38 were interactive can be reconciled with the X-ray crystal structure data for cAPK, the kinetic data for cAPK support independent peptide and ATP binding sites (Cook et al., 1982; Whitehouse et al., 1983; Kong & Cook, 1988).

As Cook et al. (1982) reported for cAPK, many of the tyrosine kinases have been reported to proceed by a random sequential mechanism (Posner et al., 1992; Cole et al., 1994; & Boerner et al., 1995). It is unclear why p38 shows a different kinetic mechanism from these other kinases. All of these mechanisms were determined utilizing peptide substrates for the kinase of interest. In our experiments, we chose the transcription factor ATF2 as a protein substrate

for p38. Raingeaud et al. (1995) showed this protein was a good *in vitro* substrate for p38 and suggested ATF2 as a potential *in vivo* substrate for p38 as well. It is yet unclear whether the kinetic mechanism for various kinases will be affected by differences between protein and peptide substrates, but it is reasonable to believe that peptides may not provide all of the contacts that a protein substrate would. Moreover, the ATP binding domain may be inaccessible in the free enzyme form, and upon protein substrate binding, a conformational change occurs which makes the site open for ATP binding. Or perhaps, in p38, protein substrate itself forms some of the ATP binding domain. In fact, Wilson et al. (1996) have suggested from their crystal structure data of unactivated and uncomplexed p38 that the ATP and protein binding domains would have to change their orientation in order for catalysis to occur. It should be noted that any comparison between p38, cAPK, and members of the tyrosine kinase family should be taken in context of their low level of amino acid identity (approximately 20−25% with other protein kinases whose structures have been reported; Wilson et al., 1996). Indeed, Wilson et al. (1996) reported large differences in the phosphorylation lip and peptide binding channel between p38 and ERK-2 (extracellular-regulated protein kinase), a MAP kinase family member which shares 48% amino acid identity with p38. Finally, an ordered sequential kinetic mechanism for p38 where protein substrate is bound first may be linked to the mechanism of activation for p38 and may produce a conformation in p38 that gives specificity to a particular upstream kinase activator. It will be interesting to see if other MAP kinases proceed by the same kinetic mechanism as p38 or if they are more similar to cAPK.

Our results from the inhibition of p38 by two triarylimidazoles and the equilibrium binding studies (Table 2; Figure 3) are also consistent with an ordered sequential mechanism for p38 with GST-ATF2 binding first. SB 202190 and SB 203580 are both competitive with ATP. The uncompetitive inhibition between these compounds and GST-ATF2 suggests inhibitor, like ATP and AMP-PCP, preferentially binds to the E·GST-ATF2 complex. However, fitting the data to the equation for full noncompetitive inhibition yields a poorly defined $K_{is}$ term for both SB 203580 (789 ± 595 nM) and SB 202190 (347 ± 192 nM), suggesting that the triarylimidazoles may show some association with free enzyme, whereas ATP and AMP-PCP, as discussed earlier, show no association with free enzyme. The equilibrium binding studies also show that the requirement for an E·GST-ATF2 complex for ATP binding is more pronounced than that for the inhibitor. Little competition between ATP and SB 202190 is seen when p38 does not contain bound GST-ATF2 (as is the case with BSA; Figure 3). However, SB 202190 can bind to BSA-complexed p38 whereas ATP cannot. A similar result is seen for activated p38 (i.e., phosphorylated) and unactivated (nonphosphorylated) p38. That is, ATP is unable to bind to unactivated p38 whereas drug is able to bind to unactivated p38 (O'Neill et al., unpublished results). One possible explanation for the weak inhibitor binding to free enzyme is that perhaps BSA can serve a similar aid for drug binding as protein substrate does, but is unable to perform this role for ATP. It is interesting to speculate that the putative conformational changes that occur upon substrate binding have differential effects upon ATP and inhibitor binding and perhaps BSA may induce the needed effect for inhibitor only. Alternatively, it may be a combination of effects from protein substrate binding and the p38 phosphorylation state that give rise to differential binding of ATP and drug to free and bound enzyme.

Understanding the kinetic mechanism for two-substrate reactions is important for inhibitor screening. For example, since p38 exhibits an ordered sequential mechanism with protein substrate binding first, any binding assay must include substrate if one is to detect inhibitors that are competitive with ATP. In general, for the p38 case, a catalytic assay would be more appropriate because both ATP and inhibitor bind preferentially to the E·GST-ATF2 complex. In a catalytic assay, it is likely that inhibitors of both ATP and protein substrate would be detected.

In summary, we have determined the kinetic mechanism for p38 to be ordered sequential with protein substrate binding first. Moreover, ATP and AMP-PCP bind only to the E·GST-ATF2 complex. The triarylimidazoles also preferentially bind to the E·GST-ATF2 complex, but show some ability to bind to free enzyme. This indicates while similar, ATP binding and drug binding to p38 have somewhat different structural requirements. Given this mechanism, it will be interesting to compare the X-ray crystal structures of uncomplexed p38 and a ternary complex of p38·AMP-PCP·protein/peptide substrate or p38·drug·protein/peptide substrate to see what structural features are required for such a mechanism.

## ACKNOWLEDGMENT

We thank Bob Frankshun for synthesis of SB 203580 and Linda Chang for synthesis of SB 202190.

## REFERENCES

Adams, J. A., & Taylor, S. S. (1992) *Biochemistry 31*, 8516−8522.
Boerner, R. J., Barker, S. C., & Knight, W. B. (1995) *Biochemistry 34*, 16419−16423.
Bunch, T. A., Grinblat, Y., & Goldstein, L. S. B. (1988) *Nucleic Acids Res. 16*, 1043−1061.
Cole, P. A., Burn, P., Takacs, B., & Walsh, C. T. (1994) *J. Biol. Chem. 269*, 30880−30887.
Cook, P. F., Neville, M. E., Jr., Vrana, K. E., Hartl, T., & Roskoski, R., Jr. (1982) *Biochemistry 21*, 5794−5799.
Cuenda, A., Rouse, J., Doza, Y. N., Meier, R., Cohen, P., Gallagher, T. F., Young, P. R., & Lee, J. C. (1995) *FEBS Lett. 364*, 229−233.
Erneux, C., Cohen, S., & Garbers, D. L. (1983) *J. Biol. Chem. 258*, 4137−4142.
Fromm, H. J. (1979) *Methods Enzymol. 63*, 467−486.
Han, J., Lee, J.-D., Tobias, P. S., & Ulevitch, R. J. (1993) *J. Biol. Chem. 268*, 25009−25014.
Han, J., Lee, J.-D., Bibbs, L., & Ulevitch, R. J. (1994) *Science 265*, 808−811.
Johnson, N. L., Gardner, A. M., Diener, K. M., Lange-Carter, C. A., Gleavy, J., Jarpe, M. B., Minden, A., Karin, M., Zon, L. I., & Johnson, G. L. (1996) *J. Biol. Chem. 271*, 3229−3237.
Kong, C.-T, & Cook, P. F. (1988) *Biochemistry 27*, 4795−4799.
Leatherbarrow, R. J. (1992) *GraFit*, version 3.0, Erithacus Software Ltd., Staines, United Kingdom.
Lee, J. C., & Young, P. R. (1996) *J. Leukocyte Biol. 59*, 152−157.
Lee, J. C., Gadger, A. M., Griswold, D. E., Dunnington, D., Truneh, A., Votta, B., White, J. R., Young, P. R., & Bender, P. E. (1993) *Ann. N.Y. Acad. Sci. 696*, 149−170.
Lee, J. C., Laydon, J. T., McDonnell, P. C., Gallagher, T. F., Kumar, S., Green, D., McNulty, D., Blumnethal, M. J., Heys, J. R., Landvatter, S. W., Strickler, J. E., McLaughlin, M. M., Siemens, I. R., Fisher, S. M., Livi, G. P., White, J. R., Adams, J. L., & Young, P. R. (1994) *Nature 372*, 739−746.

Posner, I., Engel, M., & Levitzki, A. (1992) *J. Biol. Chem. 267*, 20638−20647.
Raingeaud, J., Gupta, S., Rogers, J. S., Dickens, M., Han, J., Ulevitch, R. J., & Davis, R. J. (1995) *J. Biol. Chem. 270*, 7420−7426.
Segel, I. H. (1975) *Enzyme Kinetics*, John Wiley & Sons, Inc., New York.
Steller, H., & Pirrotta, V. (1985) *EMBO J.* 4, 167−171.
Whitehouse, S., & Walsh, D. A. (1983) *J. Biol. Chem. 258*, 3682−3692.
Whitehouse, S., Feramisco, J. R., Casnellie, J. E., Krebs, E. G., & Walsh, D. A. (1983) *J. Biol. Chem. 258*, 3693−3701.
Wilson, K. P., Fitzgibbon, M. J., Caron, P. R., Griffith, J. P., Chen, W., McCaffrey, P. G., Chambers, S. P., & Su, S.-S. M. (1996) *J. Biol. Chem. 271*, 27696−27700.
Zheng, J., Knighton, D. R., Ten Eyck, L. T., Karlsson, R., Xuong, N., Taylor, S. S., & Sowadski, J. M. (1993) *Biochemistry 32*, 2154−2161.

BI9706778